Journal of Microelectronics and Electronic Packaging (2014) **11**, 122-127

ISSN: 1551-4897

Capacitive Fringing Field Moisture Sensors Implemented in Flexible Printed Circuit Board Technology

Robert N. Dean,* Michael C. Hamilton, and Michael E. Baginski

***Abstract*—Capacitive fringing field sensors are often used in applications where moisture is detected, since the dielectric constant of liquid water is approximately 80 times greater than the dielectric constant of air. Most of these sensors, however, are realized using rigid substrates. Some applications would benefit from using a flexible capacitive fringing field sensor that could be conformally mounted on a nonplanar surface. Flexible printed circuit board technology is a mature commercially available process for manufacturing flexible electronics. This same technology can also be used to realize flexible fringing field moisture sensors where the patterned Cu foil is used for the electrodes and the soldermask coating electrically insulates the electrodes from being electrically shorted by moisture in the detection environment. Sensors were designed and characterized through flat and bending tests in air and in water. The tests demonstrated that bending a sensor over a radius of curvature as small as 13.7 mm had no measurable impact on sensor performance in air or in water. The sensors achieved a 3:1 increase in capacitance when immersed in water compared with in air.**

***Keywords*—Capacitance transducers, flexible structures, interdigital transducers, moisture transducers, printed circuits**

Introduction

Capacitive fringing field sensors consisting of interdigitated electrode "fingers" are commonly used to detect the presence of or to measure the quantity present of a substance possessing a relative permittivity significantly greater than the relative permittivity of air [1]. In particular, this type of sensor has been used in sensing the presence of water, present in either vapor (humidity) [2], liquid (moisture) [3], or solid (ice) [4] form. Additionally, this type of sensor has been used to measure the moisture content of objects and materials, such as soil [5], paper pulp [6], grain [7], wood [8], and animal hides [9]. Other applications include the measurement of water level [10], environmental parameters [11], and pH [12], and as biosensors for meat inspection [13].

Many of these implementations of fringing field sensors are on rigid substrates, which is preferred for applications such as soil moisture measurement where the electrodes must be pushed into the soil [14] and electrode deformation would be deleterious. However, other applications benefit from sensor implementations on flexible substrates where it is advantageous to conformally mount the sensor or sensor array directly onto a nonplanar surface [2, 15]. Rigid printed circuit board technology has recently been demonstrated as a suitable technology for implementing low-cost, physically large capacitive fringing field sensors for applications involving moisture measurement [3, 5]. Flexible printed circuit board technology (FPCB) is a mature, commercially available technology. It is therefore an attractive technology for realizing flexible capacitive fringing field sensors for applications involving moisture measurement. In this paper, this is demonstrated through the realization and testing of flexible capacitive fringing field moisture sensors implemented in FPCB technology.

The manuscript was received on January 2, 2014; revision received on April 17, 2014; accepted on April 18, 2014

Auburn University, Auburn, Alabama 36849
*Corresponding author; email: deanron@auburn.edu

Background

A. Capacitive Fringing Field Sensing Structures

Consider the simplistic drawing of a two-electrode capacitive fringing field sensor mounted on a nonconductive substrate in Fig. 1.

The electrodes, A and B, are at different voltage potentials. The dashed lines represent the streamlines of electric flux between A and B. When the distance between the two electrodes is much smaller than the height of the electrodes, and the width of the electrodes is negligible, most of the capacitance is a result of the electric flux linkage between the opposing faces of A and B. However, if the separation distance between the electrodes is much greater than the electrode height, a significant amount of the capacitance between A and B is directly linked to the electric flux coupled by the fringing fields outside of the volume between the electrodes. Therefore, when an object or material possessing a different dielectric constant is brought into the volume of interaction with the fringing fields, the capacitance between the two electrodes changes in proportion to that interaction and is measurable. A common application involves the sensing of water-based objects placed in the proximity of the electrodes. Since the ratio of the dielectric constant of water to air is approximately 80:1 at room temperature, a significant change in capacitance will be observed [16]. This technique assumes that the conductive media containing water does not possess a low impedance connection to ground so that shielding does not occur [17]. Also, the streamlines extend into the substrate below the electrodes, as indicated in Fig. 1, to a degree that is determined by the substrate material and thickness and any materials or structures added to the substrate backside.

doi:10.4071/imaps.415

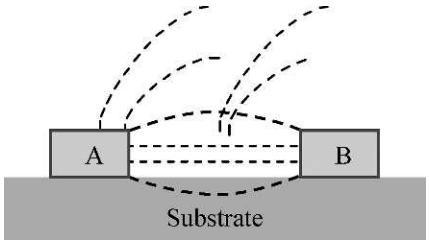

Fig. 1. A representative drawing of a two electrode fringing field sensor.

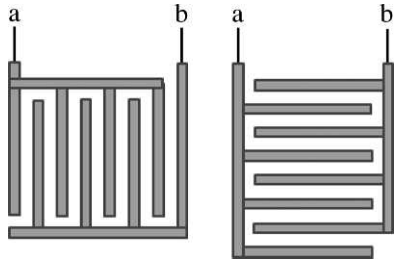

Fig. 2. Top-view illustration of two interdigitated electrodes: (a) vertical array, and (b) horizontal array.

Many capacitive fringing field sensor electrode designs have been developed for various applications. One implementation for measuring soil moisture content uses a rigid pole with two annular ring electrodes mounted concentrically [18]. Another technique utilizes two or more rigid metal rods as the electrodes for measuring soil moisture [19]. Many applications, however, utilize a planar electrode configuration where the electrodes are arrayed as parallel fingers on a nonconductive substrate [20-22]. Another electrode configuration for fringing field sensing is a two-dimensional array of metal electrode islands [23]. Rigid printed circuit board (PCB) technology has recently been demonstrated for realizing low-cost, small or large area, capacitive fringing field sensors where an FR-4 laminate was used as the rigid nonconductive substrate. Patterned Cu foil was used to realize an array of interdigitated electrode fingers and the soldermask was necessary to insulate the electrodes from moisture and other conducting fluids [5].

B. Flexible PCB Technology

FPCB technology is similar to rigid PCB technology. The primary difference is that the substrate is a thin flexible material, such as the polyimide film Kapton [24] or liquid crystal polymer (LCP) [25]. FPCB material systems are similar to rigid PCBs, and FPCBs can be patterned with Cu on one or both sides, or they can be multilayered. The Cu layer is attached in the form of a thin Cu foil that is chemically patterned as desired. A soldermask is also used on the outer Cu layer(s) to limit the flow of molten solder during electronics attachment. Bare Cu is usually coated with a suitable surface finish, depending on the application, such as HASL or immersion Sn. Many thorough references exist for FPCB technology [26].

Fringing Field Sensors in Flexible PCB Technology

A two-layer commercial FPCB process was used to implement flexible capacitive fringing field sensors. Two sensor models were implemented, horizontally arrayed and vertically arrayed, as illustrated in Fig. 2. Both designs consisted of two interdigitated electrode structures with 35 electrode pairs. Each electrode finger was nominally 152.4 μm wide and 22.56 mm long. Opposing fingers were separated by 152.4 μm.

The electrodes were patterned in the top side, 35 μm thick, Cu foil layer. The substrate was 50.8 μm thick Kapton. On the backside of the substrate, a solid, electrically floating, Cu pad was implemented in the backside Cu foil. The square pad was 23.37 mm across and completely covered the sensor electrode array on the front side. Nominally 25.4 μm thick soldermask (Taiyo PSR-900 FXT series) covered the sensor array and the backside Cu pad. The thin soldermask layer protects the electrodes from shorting in the presence of liquid water while allowing the fringing fields to extend into the sensing environment. This is a significantly different architecture than used in other similar sensing structures, such as flexible humidity sensors, where the electrode coating absorbs water vapor from the surrounding air in proportion to the relative humidity and correspondingly increases the sensor capacitance [2]. The manufactured sensors were 83.82 mm long and 26.67 mm wide. The sensor active area, approximately 23 mm by 21 mm, was located at one end of the sensor, while two electrical contact pads were located at the other end of the sensor. Photographs of the two sensors with horizontal and vertical electrode array orientations are presented in Fig. 3. On the horizontal sensor, the electrode fingers were arranged in the direction of the short dimension of the sensor. On the vertical sensor, the electrode fingers were arranged in the direction of the long dimension of the sensor.

A close-up photograph of a section of the electrode array of a vertical sensor is presented in Fig. 4. The gold colored 152.4 μm wide electrodes on a 304.8 μm pitch are clearly seen. The dark area behind and around the electrodes is the electrically floating Cu pad on the backside of the sensor as seen through the Kapton substrate. The orange area outside the dark backside Cu pad is the soldermask covered Kapton substrate outside of the sensor's

Fig. 3. Photograph of the horizontally arrayed sensor (left) and the vertically arrayed sensor (right).

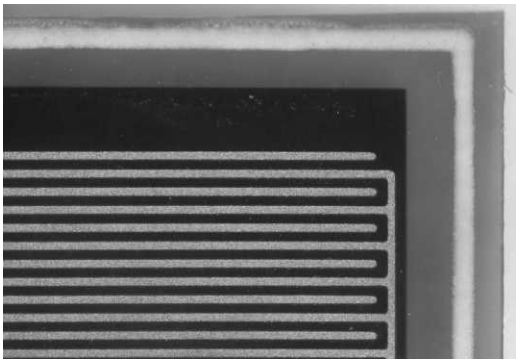

Fig. 4. Close-up photograph of a section of the electrode array for a vertical sensor.

active area. The white line is the silk screen around the sensor's active area.

Theoretical Discussion

Operation of the sensor is based on a change in total electric flux associated with the fringing field when an object of different dielectric constant is placed in the proximity of the sensor's electrodes, in the volume of the fringing fields outside of the soldermask layer. For this type of sensor to work effectively, a sufficient portion of the electric flux must penetrate into the region beyond the soldermask and other resident buffer layers. Because of the complexity of the problem, no empirical solution is available for the electric field mapping and numerical simulations are required.

ANSYS Q3D Extractor was used to investigate the electric field mapping and the effect that flexing the sensor would have on capacitance. The simulations are based on a finite element model of the region that assumes a quasi-static field distribution.

The region is assumed to be lossless and the electric field is given by the Laplace equation,

$$\nabla^2 V = 0, \tag{1}$$

$$\vec{E} = -\nabla V, \tag{2}$$

where V is the voltage and **E** is the electric field. For these simulations, all conducting surfaces were approximated as perfect electric conductors and the continuity of the normal component of the electric flux density (D_n),

$$\vec{D}_n = \vec{\varepsilon}\vec{E}_n, \tag{3}$$

was maintained at the soldermask to test the material dielectric-air interface,

$$\vec{\varepsilon}_1 \frac{\partial V}{\partial n} = \vec{\varepsilon}_2 \frac{\partial V}{\partial n}. \tag{4}$$

A plot of the normalized electric field mapping in the vicinity of the electrode fingers for a planar and flexed sensor are shown in Figs. 5 and 6, respectively. It is evident that a significant portion of the electric flux penetrates into the region adjacent to the electrode for a structure with a thin soldermask.

The effect of adding a buffer layer (i.e., soldermask or an additional insulator) on the sensor electrodes was also investigated. In Fig. 7, simulation results for fringing field sensors with varying buffer layer thickness that is surrounded by air or water is shown. Note that for thin buffer layers (a thickness less than approximately the distance between the interdigitated electrodes), the material outside the sensor structure can be detected. However, above a certain thickness of buffer layer, essentially no detection is possible, because the fringing field is contained within, and therefore the capacitance is solely determined by, the buffer layer. A key feature of Fig. 7 is that it clearly shows the significant change in capacitance that occurs when objects of different permittivities are placed in close proximity to the electrodes.

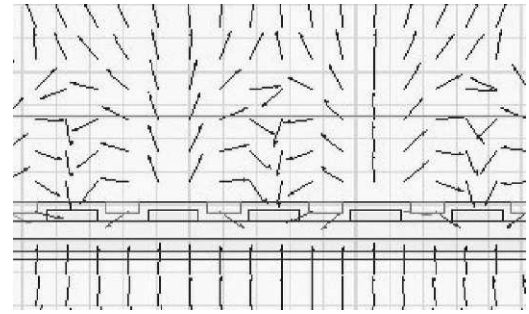

Fig. 5. Electric field mapping in the vicinity of the electrodes with a flat sensor immersed in water.

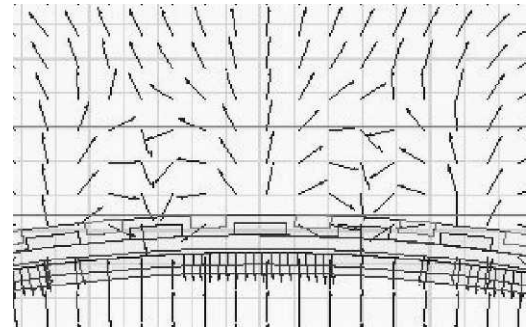

Fig. 6. Electric field mapping in the vicinity of the electrodes with a flexed sensor immersed in water.

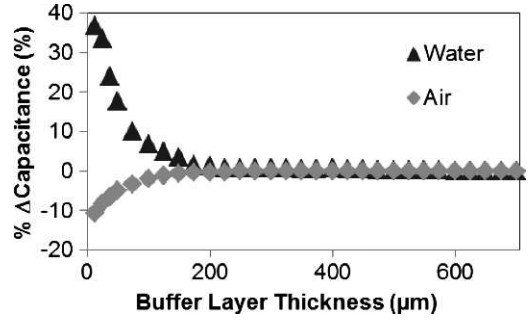

Fig. 7. Capacitance versus buffer layer thickness for sensors in water and in air.

Experimental Validation

A panel of 16 sensors was fabricated, consisting of eight horizontal sensors (H_1-H_7 and H_N) and eight vertical sensors

(V_1-V_7 and V_N) using a commercial FPCB manufacturing process. Sensors H_1-H_7 are identical and V_1-V_7 are identical, and both sets have a soldermask coating over the sensor electrode arrays. Sensors H_N and V_N are identical to the other horizontal and vertical sensors, respectively, except that they do not have a soldermask coating over the electrode arrays. H_N and V_N were used to evaluate the effect of the soldermask on the sensor design.

A. Bending Tests

In order to evaluate the effects of bending the sensors, each of the 16 sensors was attached to sections of commercially available polyvinyl chloride (PVC) pipe of varying radius of curvature so that the sensor electrodes faced away from the pipe. A sensor was attached to a section of pipe with cellophane adhesive tape carefully applied around the periphery of the sensor's active area, with care taken not to place any tape over the electrode array. The sensor's capacitance was then measured in ambient air using a Gwinstek LCR-821 capacitance meter (100 KHz, 20 samples averaged) and recorded. The air temperature during testing was 23°C. The radii of curvature for the PVC pipes utilized in this investigation are presented in Table I. Conformally attaching a sensor to the minimum radius pipe section did not plastically deform the sensor, that is, it returned to its original shape after removal from the pipe.

A photograph of a vertical sensor attached to a 50.7 mm radius (Sample Number 2) PVC pipe section for testing is presented in Fig. 8. For all tests, the vertical sensors were mounted such that the electrode fingers were oriented along the straight dimension of the pipe, while the horizontal sensors were mounted such that the electrode fingers were oriented along the curvature of the pipe.

The results of these tests are presented in the plots in Figs. 9 and 10. The data reveals that the measured capacitance is essentially independent of the radius of curvature over the bending range evaluated under this test. The noise in the data is primarily due to the movement of the connection cables between the capacitance meter (measurement-to-measurement repeatability) and the sensor being tested (sensor uniformity): it was observed that changing the distance between the test instrument probes for a given sensor could produce approximately 1 pF of change in the capacitance measurement. For each sensor (H_1-H_7, H_N, V_1-N_7, and V_N) evaluated over all conditions, the standard deviation varied from 0.037 pF to 0.31 pF. For the horizontal sensors with soldermask (H_1-H_7), the average capacitance was 69.35 pF with a standard deviation of 0.50 pF. For the vertical sensors with soldermask (V_1-V_7), the average

Table I
PVC Pipe Characteristics

Sample number	Radius of curvature (mm)
1	13.7
2	16.7
3	20.4
4	25.0
5	28.2
6	34.4
7	50.7
8	64.1
9	Flat

Fig. 8. A photograph of a vertical sensor mounted on a 50.7 mm radius PVC pipe section for testing.

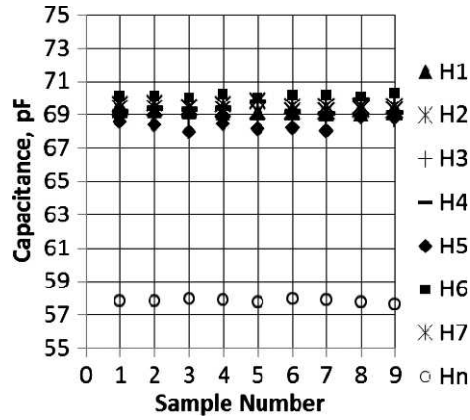

Fig. 9. A plot of the measured capacitance of the horizontally aligned sensors versus sample number from Table I.

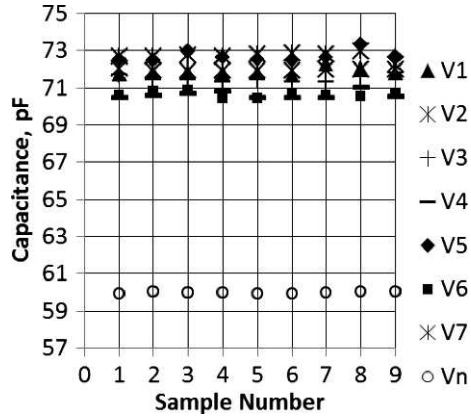

Fig. 10. A plot of the measured capacitance of the vertically aligned sensors versus sample number from Table I.

capacitance was 71.71 pF with a standard deviation of 0.80 pF. The difference in the average measured capacitance between the vertical and horizontal sensors is attributed to the traces that run from the electrode array to the connection points. These traces on the vertical sensors are slightly closer to each other than on the horizontal sensors, and hence have a slightly higher capacitance between them that adds to the capacitance from the electrode array.

The sensors without soldermask over the electrode arrays, H_N and V_N, have slightly lower measured capacitances than the otherwise identical sensors with soldermask. Specifically, the average measured capacitance for H_N was 11.4 pF less than the average measured capacitance for sensors H_1 through H_7. Similarly, the average measured capacitance for V_N was 11.7 pF less than the average measured capacitance for sensors V_1 through V_7. Although the dielectric constant for the nominally 25.4 μm thick soldermask was not known by the manufacturer, it is clearly greater than one and accounts for the approximately 11 pF increase in capacitance in the sensors with soldermask coating the electrode arrays. In simulations, the soldermask was assumed to have the same dielectric constant as that of polyimide (approximately 3.5). The purpose of the soldermask is explained in the next section.

B. Air and Water Immersion Tests

Many of the applications of this type of sensor involve direct contact with moisture [3-11]. If the electrode arrays are not coated with a thin nonconducting layer, the high conductivity of water would effectively short the electrodes. Therefore the thin coating of soldermask is necessary to allow the sensor to function in applications involving direct contact with moisture. To evaluate how well the sensor concept performs in water, one horizontal sensor and one vertical sensor with soldermask were evaluated in air and immersed in tap water, while conformally mounted to the flat PVC pipe and to the 13.7 mm radius pipe, respectively, as previously tested. For this test, the air and water temperature were both approximately 22°C, and the Gwinstek LCR-821 capacitance meter (100 KHz, 20 samples averaged) was used to measure capacitance. The resulting test data are presented in Table II.

For the horizontal sensor, the ratio of measured capacitance in water compared with in air was approximately 3.2:1. Similarly, for the vertical sensor, the ratio of measured capacitance in water compared with in air was approximately 3.0:1. The difference between the horizontal and vertical sensors is consistent with the data obtained in the bending tests. This test demonstrates that the FPCB technology capacitive fringing field sensors are suitable for use in applications where the sensor will be in direct contact with moisture and where the sensor may need to be conformally mounted on a nonplanar surface.

Table II
Results of Air and Water Immersion Tests

Sensor	Cap in air (pF)	Cap in water (pF)
H-flat	69.4	222.3
H-curved	70.3	223.1
V-flat	71.9	214.7
V-curved	72.44	216.51

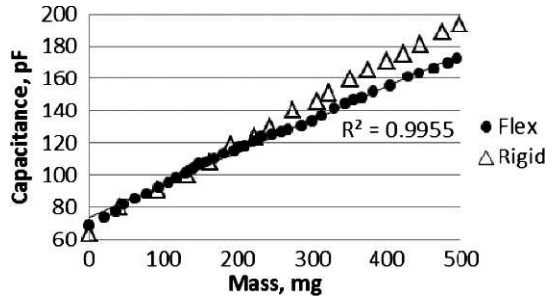

Fig. 11. A plot of the measured capacitance versus mass of added water for the rigid sensor [1] and the flexible sensor.

Comparison with Published Research

A previously published rigid PCB fabricated sensor of the same design was used to measure the mass of added drops of water and to measure the moisture content of soil [1]. Therefore a flexible sensor was also evaluated by measuring the mass of added water and compared with the rigid sensor's published data. The flexible sensor utilized the same interdigitated electrode design as the rigid sensor and it was tested in exactly the same fashion as the rigid sensor was. The flexible sensor was mounted on an Acculab VIC-123 precision digital scale and connected to a Gwinstek LCR-821M to measure capacitance. Then small drops of water were incrementally added to the sensor's active area. The surface of the sensor's active area was mostly hydrophobic such that the water beaded up on the surface. Successive drops were added to the previous drop toward the center of the sensing element such that a single drop became larger with each added quantity of water. The mass of the cumulative water after each added drop and the sensor's output capacitance were measured after short-term stabilization of the reading was achieved. Long-term stabilization of capacitance readings, such as due to possible polyimide absorption of moisture, was not evaluated in this study. The resulting data are presented in Fig. 11 along with the published data from the rigid sensor [1]. Both sensors possessed the same characteristic trend. For linear fits to the measured data, the data for the rigid sensor had an R^2 value of 0.9982 while the data for the flexible sensor had an R^2 value of 0.9955, indicating a nearly linear sensor response. This experiment verifies that the FPCB sensor possesses the same operating characteristics as the rigid PCB sensor.

Conclusions

Capacitive fringing field sensors are utilized in many sensing applications involving moisture detection. Numerous versions of rigid and flexible sensors have been developed for these applications. Recently, a commercially available rigid PCB process was demonstrated for realizing a low-cost version of this type of sensor. Some applications, however, require a flexible sensor that can be conformally mounted to a nonplaner surface and provide electrical isolation of the sensing electrodes from the operating environment. Flexible PCB technology is well suited for implementing flexible capacitive fringing field

sensors. This was demonstrated using a commercially available flexible PCB process where the sensor architecture was optimized for applications involving liquid water using the materials and processes available in a commercial flexible PCB process. The resulting sensors were successfully characterized in air and in water, and by conformally mounting the sensors to PVC pipe sections of various radii of curvature. Flexible sensor performance was compared with the published data from tests of rigid PCB sensors of the same electrode array design verifying almost identical operating characteristics.

References

[1] A.V. Mamishev, K. Sundara-Rajan, F. Yang, Y. Du, and M. Zahn, "Interdigital sensors and transducers," *Proceedings of the IEEE*, Vol. 92, No. 5, pp. 808-845, 2004.

[2] J. Laconte, V. Wilmart, J.-P. Raskin, and D. Flandre, "Capacitive humidity sensor using a polyimide sensing film," Proceedings of the 2003 Design, Test, Integration & Packaging of MEMS/MOEMS Conference, pp. 223-228, 5-7 May 2003.

[3] R.N. Dean and A.K. Rane, "A digital frequency-locked loop system for capacitance measurement," *IEEE Transactions on Instrumentation and Measurement*, Vol. 62, No. 4, 777-784, 2013.

[4] X.M. Chang, Y. Dou, D. Zhuo, and J.H. Fan, "Research on sensor of ice layer thickness based on effect of fringe electric field," Proceedings of the 2012 IEEE International Conference on Computing, Measurement, Control and Sensor Network, pp. 417-420, 7-9 July 2012.

[5] R.N. Dean, A. Rane, M. Baginski, J. Richard, Z. Hartzog, and D.J. Elton, "A capacitive fringing field sensor design for moisture measurement based on printed circuit board technology," *IEEE Transactions on Instrumentation and Measurement*, Vol. 61, No. 4, pp. 1105-1112, 2012.

[6] K. Sundara-Rajan, L. Byrd, II, and A.V. Mamishev, "Moisture content estimation in paper pulp using fringing field impedance spectroscopy," *IEEE Sensors Journal*, Vol. 4, No. 3, pp. 378-383, 2004.

[7] R.B. McIntosh and M. Casada, "Fringing field capacitance sensor for measuring the moisture content of agricultural commodities," *IEEE Sensors Journal*, Vol. 8, No. 3, pp. 240-247, 2008.

[8] Z. Liu, S. Liu, Y. Luo, J. Wang, and S. Wang, "Permittivity measurement of wood based on an unipolar capacitance sensor," Proceedings of the IEEE International Conference on Information and Automation, pp. 912-916, 20-23 June 2010.

[9] M.A.M. Yunus, V. Kasturi, S.C. Mukhopadhyay, and G.S. Gupta, "Sheep skin property estimation using a low-cost planar sensor," Proceedings of the IEEE International Instrumentation and Measurement Technology Conference, 5-7 May 2009.

[10] Y.-T. Li, C.-M. Chao, and K. Wang, "A capacitance level sensor design and sensor signal enhancement," Proceedings of the 6th IEEE International Conference on Nano/Micro Engineered and molecular Systems, pp. 847-850, 20-23 Feb. 2011.

[11] M.A.M. Yunis and S.C. Mukhopadhyay, "Development of planar electromagnetic sensors for measurement and monitoring of environmental parameters," *Measurement Science and Technology*, Vol. 22, No. 2, p. 025107, 2011.

[12] A. Manut, A.S. Zoolfakar, R.A. Rani, and M. Zolkapli, "Mechanical parameters characterization of planar FEF fingers for pH sensor," Proceedings of the 2011 International Conference on Electron Devices, Systems and Applications, pp. 191-194, 3-7 Dec. 2011.

[13] S.C. Mukhopadhyay and C.P. Gooneratne, "A novel planar-type biosensor for noninvasive meat inspection," *IEEE Sensors Journal*, Vol. 7, No. 9, pp. 1340-1346, 2007.

[14] D. Wobschall and D. Lakshmanan, "Wireless soil moisture sensor based on fringing capacitance," Proceedings of the 2005 IEEE Sensors Conference, pp. 8–11, 2005.

[15] N. Chen, J. Engel, J. Chen, Z. Fan, and C. Liu, "Micromachined thermal imaging mesh for conformal sensing system," Proceedings of the 2005 IEEE Sensors Conference, pp. 700-703, 30 Oct.-3 Nov. 2005.

[16] W.H. Hayt, *Engineering Electromagnetics* (p. 508), McGraw-Hill, New York, 1981.

[17] M. Tartagni and R. Guerrieri, "A fingerprint sensor based on the feedback capacitive sensing scheme," *IEEE Journal of Solid-State Circuits*, Vol. 33, No. 1, pp. 133-142, 1998.

[18] J.P. Bell, T.J. Dean, and M.G. Hodnett, "Soil moisture measurement by an improved capacitance technique, Part II. Field techniques, evaluation and calibration," *Journal of Hydrology (Amsterdam)*, Vol. 93, pp. 79-90, 1987.

[19] H. Eller and A. Denoth, "A capacitive soil moisture sensor," *Journal of Hydrology (Amsterdam)*, Vol. 185, pp. 137-146, 1996.

[20] S. Sulaiman, A. Manut, and A.R. Nur Firdaus, "Design, fabrication and testing of fringing electric field soil moisture sensor for wireless precision agriculture applications," Proceedings of the 2009 IEEE International Conference on Information and Multimedia Technology, pp. 513-516, 16-18 Dec. 2009.

[21] A.V. Mamishev, K. Sundara-Raijan, F. Yang, Y. Du, and M. Zahn, "Interdigital sensors and transducers," *Proceedings of the IEEE*, Vol. 92, No. 5, pp. 808-845, 2004.

[22] M.N. Alam, R.H. Bhuiyan, R.A. Dougal, and M. Ali, "Concrete moisture content measurement using interdigitated near-field sensors," *IEEE Sensors Journal*, Vol. 10, No. 7, pp. 1243-1248, 2010.

[23] Y.-T. Li, Y.-L. Tzeng, C.-M. Chao, and K. Wang, "Electrode design optimization of a CMOS fringing-field capacitive sensor," Proceedings of the 7th IEEE International Conference on Nano/Micro Engineered and Molecular Systems, pp. 603-606, 5-8 March 2012.

[24] M.A. Aziz, S. Roy, L.A. Berge, and S. Irfanullah, Nariyal and B.D. Braaten, "A conformal CPW folded slot antenna array printed on a Kapton substrate," Proceedings of the IEEE 6th European Conference on Antennas and Propagation, pp. 159-162, 26-30 March 2012.

[25] R. Dean, J. Weller, M. Bozack, C. Rodekohr, B. Farrell, L. Jauniskis, J. Ting, D. Edell, and J. Hetke, "Realization of ultra fine pitch traces on LCP substrates," *IEEE Transactions on Components and Packaging Technologies*, Vol. 31, No. 2, pp. 315-321, 2008.

[26] T.H. Sterns, *Flexible Printed Circuitry*, McGraw-Hill, New York, 1996.